Desalination and Water Treatment
www.deswater.com

doi: 10.1080/19443994.2013.795875

52 (2014) 2560–2571
March

Taylor & Francis
Taylor & Francis Group

Adsorption properties of aqueous ferric ion on natural cotton fiber: kinetic and thermodynamic studies

Mohammed A. Al-Anber[1]

Department of Chemical Sciences, Faculty of Sciences, Mutah University, P.O.Box 7, Karak, 61710, Jordan
Tel: +962 (0) 777 2128 17; email: masachem@mutah.edu.jo

Received 4 December 2012; Accepted 8 April 2013

ABSTRACT

The aqueous ferric (Fe^{3+}) ion has been successfully adsorbed by natural cotton fibers (NCF). The equilibrium of adsorption has been carried out, by taking into account the influence of the ferric ion concentration, doses of NCF, temperature, and the contact time. The percentage of adsorption is slightly increased while increasing the temperature. Langmuir and Freundlich adsorption models are applied in order to describe the thermodynamic parameters and to understand the sorption behavior of ferric ion onto NCF. The Fe^{3+}−NCF adsorption system follows Langmuir and Freundlich isotherm models ($R^2 > 0.993$). The capacity (q_{max}) and intensity (b) of Langmuir adsorption are calculated to be 49.75 mg g^{-1} and 0.0193 L mol^{-1}, respectively. The capacity (K_f) and intensity ($1/n$) of Freundlich adsorption are 1.114 and 0.840, respectively. The results reveal that the adsorption of ferric ion on NCF is chemisorption, spontaneous and favorable in nature. Adsorption reaction kinetic models, such as pseudo-first-order and pseudo-second-order, and adsorption diffusion model, such as Weber–Morris intra-particle diffusion model, have been used to describe the adsorption rate and mechanism of the ferric ion onto NCF surface. The Fe^{3+}−NCF adsorption system has achieved Lagergren pseudo-second-order model ($R^2 = 1.0$ approx.). The kinetic parameters, rate constant, and sorption capacities are calculated. These results suggest that NCF has a high potential use in the removal of ferric ion from aquatic systems.

Keywords: Ferric ion; Cotton; Sorption; Langmuir and Freundlich; Kinetic; Pseudo-second-order

1. Introduction

Most pollutants and hazardous substances are of concern because of their toxic effect. It is possible to classify the heavy metals as toxic water pollutants. Because of the toxicity of many heavy metals, their concentrations must be reduced in the aqueous system to very low level in order to protect human health and environment [1–2]. Iron is found in the water froms due to a number of industrial processes such as, corrosion of galvanized or steel plumbing materials. From other hand, iron can be dissolved from soils and rocks as the water passes through the earth. A small amount of iron ions affects the usefulness of the water for household purposes. Its presence in the concentrations greater than 0.3 mg L^{-1} stains plumbing fixtures and laundered clothes. It

[1]Current address: Department of Environmental Health, Faculty of Public Health and Health Informatics, Hail University, Hail, Saudi Arabia, Tel. +966 (0)5 40831976.

causes a foul-metallic taste and odor, rising with the growth of iron bacteria [3]. Furthermore, the presence of iron ion in a high-level causes anorexia, oliguria, diarrhea, hypothermia, dysphasic shock, and metabolic acidosis [4]. However, due to the health and industrial consideration, iron ions must be removed or decreased to the recommended healthy-level in the aquatic system.

A number of approaches are used for removing iron ion. The most common approaches are physical–chemical treatment technologies such as supercritical fluid extraction, bioremediation, oxidation, and adsorption processes [5–7]. Adsorption is considered to be the most economic and efficient process that can be used. Particularly, special attention has been directed towards the usage of natural organic or inorganic adsorbents for the removal of iron ions, such as zeolite [8], activated carbon [9], olive cake (OC) [10], Bengal gram husk powder [11], quartz, and bentonite [12], banana ash [13], coal [14], chitin [15], and chitosan [16,17]. To investigate the adsorption behavior of the ferric ion on these adsorbents, several thermodynamics and kinetics models have been applied.

Natural cotton fiber (NCF) is considered to be natural adsorbents that could be used to remove metallic ion from the water system. In chemical terms, NCF consist of 95% cellulose with reactive carboxylic and hydroxyl functional groups [18–20]. Wherein, the electrostatic interactions between the functional group and the metal ion cause these groups to react readily. Therefore, these hydroxyl groups become active binding sites for adsorbing metal ion. However, there is a good number of research for removing a heavy metal from the aquatic system by using pure-cellulose, cellulose-containing materials, and modified-cellulose [21–25]. Swelling and dissolution mechanism of regenerated cellulosic fibers in the aqueous alkaline solution containing ferric–tartaric acid complex have been recently reported [26,27]. But in general, it is known that the cellulosic fibers have a weak ability of adsorbing heavy metal ions [28].

To my best knowledge, no study has been reported concerning the adsorption behavior of aqueous ferric ion on NCF. Therefore, the main objective of this study is the usage of NCF as a low cost adsorbent to remove a high-level of the aqueous ferric ion from the polluted model solution. The parameters of the adsorption process by NCF were investigated. These parameters included a dose of adsorbent, initial concentration of ferric ion in the solution, temperature, and contact time of exposure. The sorption process was modeled by thermodynamic (e.g. Langmuir and Freundlich) and kinetic (pseudo-first-order and pseudo-second-order) models.

2. Material and methods

2.1. NCF

NCF was taken from Al-Helal Cotton Factory (Al-Hassan industrial city/Jordan). The major portions of the noncellulosic compounds were wax, pectin substances, organic acids, sugars, and ash [29]. Cotton wax was found on the outer surface of NCF. This wax was removed by washing the fibers in warm *n*-hexane solvent. After chemical processing of cotton fibers (by using an alkali solution of NaOH and then bleaching with H_2O_2), all these noncellulosic materials were removed and the cellulose content of the cotton fibers was over by 99%. The washing process of NCF was done by using hot distilled water (less than 93°C) with a wetting agent in water-to-fibers ratio 15:1 for 3 h. The dried NCF was used. Each 2 g of cotton fibers has 0.2% ash and 0.34% total solids. The FT-IR spectrum showed major peaks at 1,636 and 3,300 cm^{-1} that related to the stretching frequency of the carboxylic and hydroxyl functional group, respectively.

2.2. Reagents

All chemicals were of as analytical grade and used as received. $Fe(NO_3)_3{\cdot}6H_2O$ was purchased from Fluka AG (Buchs, Switzerland). NaOH (0.1 mol L^{-1}), HNO_3 (0.1 mol L^{-1}), H_2O_2 (0.1 mol L^{-1}), and HCl (0.1 mol L^{-1}) were purchased from Merck (Darmstadt, Germany). A stock solution of Fe^{3+} ions was prepared by dissolving 6.33 g $Fe(NO_3)_3{\cdot}6\ H_2O$ (±0.01 g) in 1,000 mL ultrapure deionised water (18 Ω cm). Standard ferric ion solutions of 50, 100, 150, and 200 mg L^{-1} were prepared by appropriate dilution. The initial pH of the solution was adjusted using 1% HNO_3 for all experiment runs.

2.3. Apparatus and instruments

Atomic Absorption Spectrophotometer (Model AA 100, Perkin-Elmer), was used to analyze the ferric ion concentration in aqueous solution. Conductivity and pH were measured using a handheld conductivity meter (4520-Jenway) and a handheld pH meter (350-Jenway), respectively. The temperature was controlled using an isothermal shaker (Isothermal Gefellschaft Fur 978, ± 0.1°C). An analytical balance was used with an accuracy of ±0.0001 mg (Model of Sartorius, CP324-S, management system certified according to ISO 9001).

2.4. Equilibrium studies

The uptake of ferric ion was calculated from the mass balance, which was stated as the amount of

ferric ion adsorbed onto NCF. It equals the amount of ferric ion removed from the aqueous solution. Mathematically, it can be expressed by Eqs. (1)–(2) [30]:

$$q_e = \frac{(C_i - C_e)}{S} \quad (1)$$

$$q_t = \frac{(C_i - C_t)}{S} \quad (2)$$

where q_e is the ferric ion amount adsorbed on the NCF surface at equilibrium (mg g^{-1}), q_t is the ferric ion amount adsorbed on the NCF surface at a specific time (mg g^{-1}), C_i is the initial concentration of ferric ion in the aqueous solution (mg L^{-1}), C_e is the equilibrium concentration or final concentration of ferric ion in the aqueous solution (mg L^{-1}), and C_t is the final concentration of ferric ion in the aqueous solution (mg L^{-1}) at a specific time, t.

The dosage (slurry), S, concentration of NCF is expressed by Eq. (3):

$$S = \frac{m}{v} \quad (3)$$

where v is the initial volume of ferric ion solution used (L) and m is the mass of NCF adsorbent.

The adsorption percentages (%) are calculated by Eq. (4):

$$\%\ \text{adsorption} = \frac{C_i - C_e}{C_i} \times 100\% \quad (4)$$

The simplest and most common method of estimating contaminant retardation is based on the distribution coefficient, K_d. The K_d parameter is a factor related to the partitioning of a contaminant (Fe^{3+} ions) between the solid (NCF adsorbent) and aqueous phases. The partition coefficient, K_d, is defined as the ratio of ferric ion quantity that adsorbed per mass of NCF to the amount of ferric ions remaining in the solution at equilibrium. For the chemical reaction in the Scheme 1,

The distribution ratio (K_d) is calculated by using Eq. (5):

$$K_d = \frac{\text{amount of Fe(III) in adsorbent}}{\text{amount of Fe(III) in solution}} \times \frac{1}{S} \quad (5)$$

Furthermore, the adsorption percentages and K_d (L g^{-1}) are correlated by Eq. (6) [31]:

$$\%\ \text{adsorption} = \frac{100K_d}{K_d + 1/S} \quad (6)$$

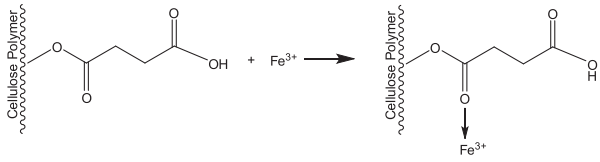

Scheme.1. Schematic representation for the chemisorptions of ferric ion on NCF.

2.5. Effect of dosage

The adsorption experiments were carried out by a batch technique at a temperature of 30°C (±1°C). Different doses of NCF (6, 10, 20, and 30 g L^{-1}) were placed in a 100 mL stopper plastic flask containing 50 mL of aqueous ferric ion (C_i = 100 mg L^{-1}). The solutions were shaken vigorously by using thermostatic mechanical shaker for 3.0 h. The agitation speed (300 rpm) was kept constant for each run to ensure equal mixing. At the end of the equilibrium, the flasks were removed from the shaker, and then the solution was filtered using a filter paper (Whatman No. 41). The filtrate supernatant solutions were analyzed. All the reported results were the average of the at least triplicate measurements.

2.6. Effect of contact time

The adsorption experiments were carried out by a batch technique at a temperature of 30°C (±1°C). The stopper plastic flasks containing 50 mL of initial concentrations (C_i = 100 mg L^{-1}) of ferric ion and 10 g L^{-1} of NCF were shaken vigorously by using thermostatic mechanical shaker (300 rpm) for a known period in the interval of 5–180 min. The flasks were removed from the shaker each 10 min up to 60 min, each 30 min up to 120 min, and finally each 60 min up to 180 min. At the end of the predetermined interval, the NCF solid was filtered using filter paper (Whatman No. 41). The filtrate supernatant solutions were analyzed. All the reported results were the average of the at least triplicate measurements.

2.7. Effect of the initial concentration

The adsorption experiments were carried out by a batch technique at a temperature of 30°C (±1°C). The stopper plastic flasks containing 50 mL of different initial concentrations (C_i = 30, 50, 100, 150 and 200 mg L^{-1}) of ferric ion and 10 g L^{-1} of NCF were shaken vigorously by using thermostatic mechanical shaker for 3.0 h. The agitation speed (300 rpm) was kept constant for each run to ensure equal mixing. At the end of the equilibrium time, the flasks were removed from the shaker, and then NCF solid was filtered using filter

paper (Whatman No. 41). The filtrate supernatant solutions were analyzed. All the reported results were the average of at least triplicate measurements.

2.8. Effect of the temperature

The adsorption experiments were carried out by the stopper plastic flasks containing 50 mL of 100 mg L^{-1} of ferric ion and 10 g L^{-1} of NCF were shaking vigorously by using thermostatic mechanical shaker at constant contact time (3 h) and agitation speed (300 rpm) with varying temperatures (30, 40, and 50°C). At the end of the equilibrium time, the flasks were removed from the shaker, and then NCF solid was filtered using filter paper (Whatman No. 41). The filtrate supernatant solutions were analyzed. All the reported results were the average of at least triplicate measurements.

2.9. Isotherm and kinetic models

The isotherm experiments were conducted by using 50, 100, 150, and 200 mg L^{-1} of ferric ion solutions. The initial pH was adjusted using 1% HNO_3 solution. The mixtures containing 0.5 g NCF and 50 mL of ferric ion solutions were stirred under the shaking conditions of 300 rpm, 180 min, and 30°C. Afterwards, the flasks were removed from the shaker, and then NCF solid was filtered by the filter paper (Whatman No. 41). The filtrate supernatant solutions were analyzed. All the reported results were the average of at least triplicate measurements.

For the kinetic studies, a number of samples containing 0.5 g NCF and 50 mL of ferric ion solutions (C_i = 100 mg L^{-1}) were placed in the 100 mL flasks. The initial pH was adjusted using 1% HNO_3 solution. These flasks were agitated using a temperature-controlled shaker (T = 30°C) at 300 rpm for 180 min. Afterwards, the flasks were removed from the shaker at an interval of every 10 min in the first 60 min and then 30 min until the end of 180 min. The NCF solid was filtered using filter paper (Whatman No. 41). The filtrate supernatant solutions were analyzed. All the reported results were the average of at least triplicate measurements.

3. Results and discussions

3.1. pH and conductivity

Iron in the water bodies exists in two forms of ionic states, Fe^{+3} (ferric) and Fe^{+2} (ferrous). The latter is soluble, while the former is only soluble under highly acidic conditions. These cations can form precipitates with a variety of anions present in the water if one or both exists in high concentrations. Ferrous iron can be oxidized to the ferric state in the presence of oxygen [13]. However, it was reported that essentially no soluble ferric iron exists in the water with a pH greater than 3.5 [32]. Therefore, the standard solutions of ferric ion solutions were prepared by using 1% HNO_3 for all experiment runs. An "initial" pH and its subsequent adjustment for all experimental runs were conducted less than 1.20 at the maximum value. Thus, aqueous ferric ions cannot be precipitated as $Fe(OH)_3$. From other hand, the effect of pH on the adsorption of aqueous ferric ion cannot be studied because the aqueous ferric ion solution itself is acidic.

The aqueous ferric ion can be removed from solution by adsorption process onto NCF. To reflect this understanding, the pH information is presented in Fig. 1. It can be observed that the initial pH (= 1.15) of the initial ferric ion concentration (100 mg L^{-1}) decreased as the adsorption time increased up to 50 min, and then it almost stayed constant in the time range from 50 to 180 min. This is due to the adsorption equilibrium. It can be noted that the final pH value of ferric ion solutions was 0.65 after 180 min of sorption equilibrium.

Fig. 2 shows the conductivity of the ferric ion solution versus the adsorption time. It can be seen that the conductivity of the solution decreased as adsorption time increased at 30°C. This decline can be considered as evidence for decreasing the number of iron ions in the solution by the adsorption on NCF.

3.2. Effect of NCF doses

Experimental results of the NCF dosage effect are illustrated in Fig. 3. It was observed that the adsorp-

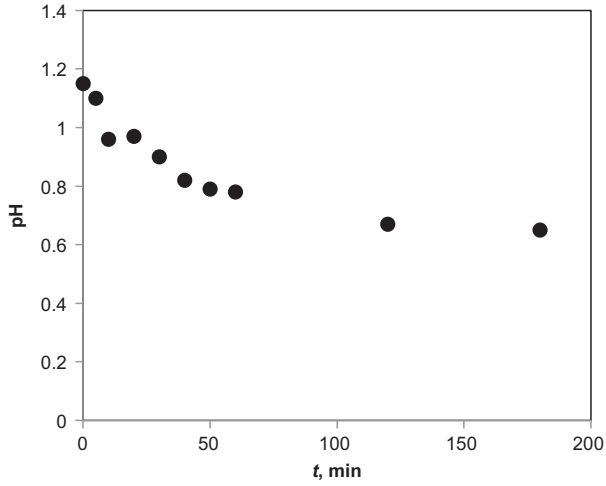

Fig. 1. Final pH values of ferric ion solution as a function of adsorption time (dose 10 mg L^{-1}; T = 30°C; 300 rpm; and C_i = 100 mg L^{-1}).

tion percentage of ferric ion increases rapidly as the NCF dosage increases. The maximum percentage removal was 90% by using 30 g L^{-1} of NCF. This is mainly due to the increase in the adsorption surface area and the numbers of available binding active sites [10–11].

A distribution coefficient, K_d, is calculated and presented as shown in Fig. 4. This coefficient reflects the binding ability of the NCF active sites of ferric ion. The K_d decreases as the dosage of NCF increases. Generally spoken, if the surface is homogeneous, it means that the value of K_d values at a given pH should not be changed with the amount "dosage" of NCF adsorbent. Therefore, the regression curve indicates the heterogeneity of NCF surface (see Fig. 4).

3.3. Effect of contact time

The influence of contact time on the adsorption of ferric ions by NCF adsorbent is shown in Fig. 5. At the initial stage of adsorption through the first 5 min, we have found a quick adsorbing and rapid uptake of ferric ion from the aqueous solution. This behavior may be due to the availability of more binding active sites that are still uncovered at the beginning of the adsorption reaction onto the NCF solids. For example, the removal of ferric ion is 75% (approx.) at the first 5 min of sorption. This stage shows that the binding active sites on NCF surface are mostly covered before 5 min. In addition, quick adsorption indicates the easy migration of ferric ion into the surface and the micropores of NCF. Therefore, this migration step is not important in the rate-controlling step of the adsorption reaction [33]. At the next stages of adsorption, a smooth and continual plot is observed leading to the saturation. This is due to the gradual decline of the remaining binding active sites on NCF. At this stage, the final equilibrium of sorption starts after 120 min (approx.), where ferric ions are slowly interacted with available active sites on the interior surface and pores of NCF adsorbent. The maximum adsorption of ferric ions occurs during the first 120 min, wherein the adsorption percentage is 90%. After this equilibrium period, the adsorbed amount of ferric ions does not significantly change with time. Similar results have been observed in many studies using different natural adsorbent such as bentonite and quartz [12,34,35], Zeolite [8,36], chitosan [16], and granular

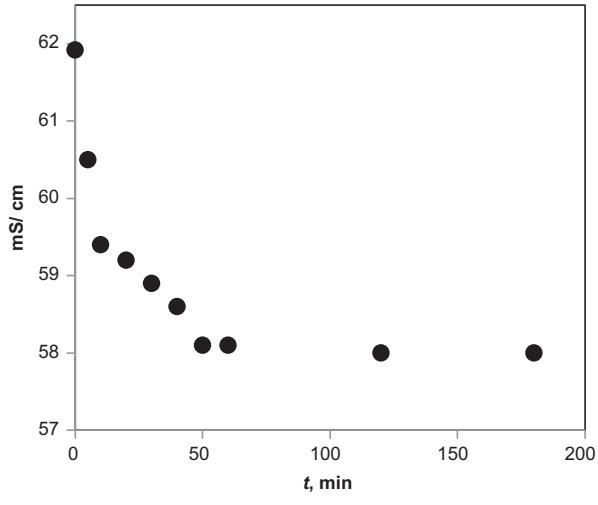

Fig. 2. Final conductivity values of ferric ion solution as a function of adsorption time (dose 10 mg L^{-1}; $T = 30°C$; 300 rpm; and $C_i = 100$ mg L^{-1}).

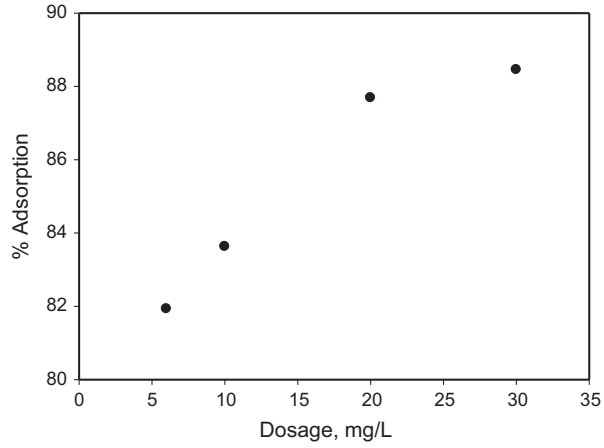

Fig. 3. The doses effect of NCF on the removal ferric ion from the aquatic system (doses: 6, 10, 20, and 30 g L^{-1}; $C_i = 100$ mg L^{-1}; $t = 3$ h; $T = 30°C$; and rpm = 300).

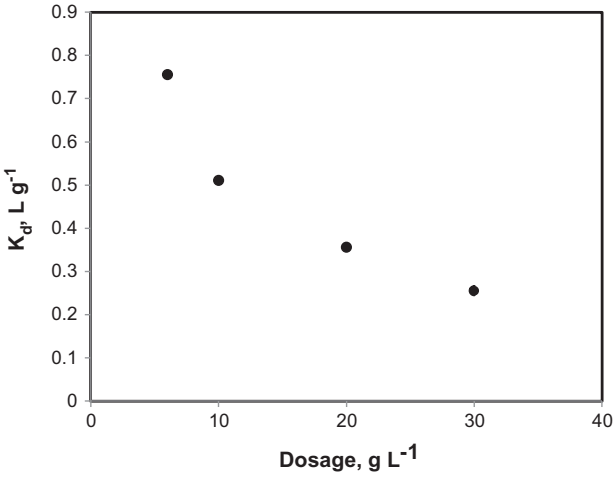

Fig. 4. The doses effect of NCF on the distribution coefficient, K_d, of ferric ion (doses: 6, 10, 20, and 30 g L^{-1}; $C_i = 100$ mg L^{-1}; $t = 3$ h; $T = 30°C$; and rpm = 300).

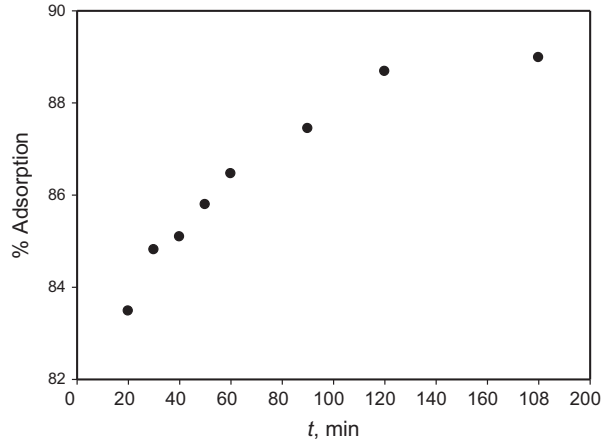

Fig. 5. The contact time effect of the adsorption reaction on the removal ferric ion from the aquatic system by NCF (t: 5 → 120 min; doses = 10 g L^{-1}; C_i = 100 mg L^{-1}; T = 30°C; and rpm = 300).

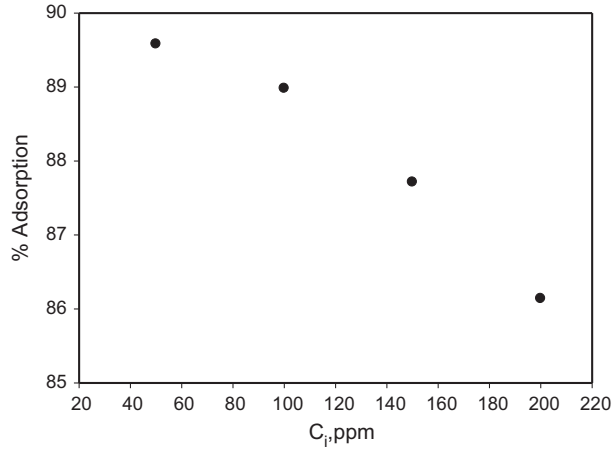

Fig. 6. The initial concentration of the aqueous ferric ion on the adsorption reaction and removal process by NCF (C_i: 30, 50, 100, 150 and 200 mg L^{-1}; doses = 10 g L^{-1}; t = 3 h; T = 30°C; and rpm = 300).

activated carbon [33]. In general, the sorption rate of ferric ion onto NCF is found lesser.

3.4. Effect of initial ferric ion concentration

The initial concentration of ferric ion plays an important role in determining the adsorption capacity of the NCF adsorbent. The adsorption percentages vs. different initial concentrations of ferric ion, viz. 50, 100, 150, and 200 mg L^{-1}, are shown in Fig. 6. The adsorption percentage increases as the initial concentration of ferric ion decreases. For example, the adsorption percentage is 90% by using 30 mg L^{-1}, while it is found 86% at high-level (200 mg L^{-1}). As we can see, the difference is not significant. At high-level concentrations, the availability of the binding active site on NCF becomes less. This behavior is connected with the competitive diffusion process of the Fe^{3+} ions onto NCF surface. This behavior leads to the plugging the inlet pores of the NCF surface, and this prevents the ferric ions to pass deeply inside. These results indicate that it is the energetically less favorable site by increasing ferric ion concentration in aqueous solution. Furthermore, the presence of high amount of ferric ion creates the aggregation of particles by the formation of the viscous emulsion, which could decrease the total surface area of NCF and an increase in diffusion path length.

3.5. Effect of temperature

The adsorption mechanism is often an important indicator to describe the type and the level of interactions between ferric ion and NCF adsorbent. To evaluate the effect of temperature for adsorbing ferric ion by NCF, the experiments are studied by using constant initial concentration (100 mg L^{-1}), dosage (10 g L^{-1}), stirring speed (300 rpm), adsorption time (180 min), and different temperatures (30, 40, and 50°C). Fig. 7 shows the effect of temperature on the adsorption of the ferric ion onto NCF adsorbent. It has been observed that the adsorption percentage increases as the temperature increases. The maximum adsorption (90%) is found at a temperature of 50°C, while it is 86% at 30°C. The adsorption of ferric ion onto the NCF surface has been found non-highly affected by raising the temperature values. It was observed that although the difference was not great, the rate of adsorption and the equilibrium adsorption increased slightly as the temperature increased (see Fig. 7). High temperature leads to an increase in the movement of iron ions in solution, and then the adsorption of ferric ions can be occurred very fast. Furthermore, higher temperatures have the ability for releasing the proton of alcohol functional group in NCF more than low temperatures, and hence ferric ion can bind with negative oxygen atom faster [37–39]. Generally, if the adsorption decreases by using higher temperature, it may be an indication of physisorption, and the reverse is generally true for chemisorptions [40]. Thus, the chemisorptions behavior of ferric ion and the higher rate of adsorption onto NCF are consistent with the previous report [12].

3.6. Isotherm modeling

Equilibrium is described by sorption isotherms, characterized by certain constants whose values express the surface properties and efficient of the

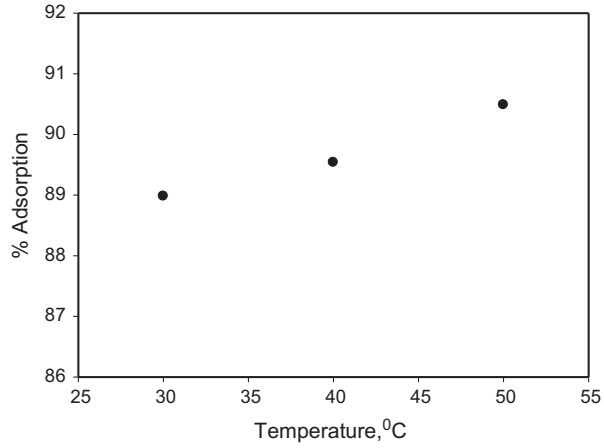

Fig. 7. The temperature effect of the adsorption reaction on the removal ferric ion from the aquatic system by NCF (T: 30, 40, and 50°C; doses = 10 g L^{-1}; C_i = 100 mg L^{-1}; t = 3 h; and rpm = 300).

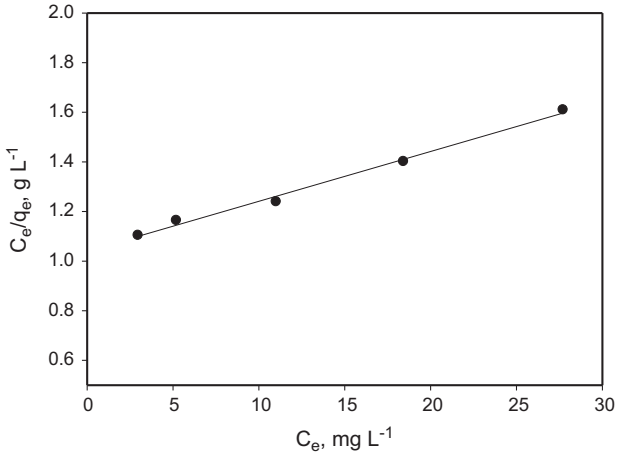

Fig. 8. The linearized Langmuir adsorption isotherms for adsorbing Fe^{3+} ion on NCF (T = 30°C; doses = 10 g L^{-1}; C_i = 100 mg L^{-1}; t = 3 h; and rpm = 300).

adsorbent. Adsorption isotherm is an invaluable curve describing the phenomenon governing the mobility of ferric ion from the aquatic system to NCF solid adsorbent at constant temperature (30°C). The experimental data for the adsorption equilibrium are analyzed by wellknown isotherms, such as the Langmuir and Freundlich sorption models. The Langmuir isotherm model is based on the monolayer coverage of the adsorbent surfaces by the adsorbate at specific homogenous sites within the adsorbent, and then no further adsorption takes place. It represents the equilibrium distribution of ferric ion between NCF and aqueous phases. The linear form of the Langmuir isotherm model is represented by Eq. (7) [41]:

$$\frac{C_e}{q_e} = \frac{1}{q_{max} b} + \frac{1}{q_{max}} C_e \quad (7)$$

A plot of C_e/q_e vs. C_e gives a straight line of slope $1/q_{max}$ and intercept ($1/q_{max}$ b) as shown in Fig. 8. It can be seen that the isotherm data have yielded excellent fits within the Langmuir isotherm, based on its correlation coefficient value (R^2 = 0.993). The value of maximum adsorption capacity, q_{max}, and adsorption affinity, b, were calculated to be 50 g kg^{-1} and 0.0193 L mg^{-1}, respectively. The calculated q_{max} and b in the laboratory scale has a good capacity of adsorbent and stronger adsorption affinity of ferric ion for adsorbing on NCF.

However, the monolayer and homogeneous adsorption and of ferric ion onto NCF was found in this work consistent with other reported results in the literatures, such as adsorption of ferric ion on the zeolite (NZ) [8], chitosan [17], palm fruit bunch and maize cob [42], carbon [9,43], and eggshell [44]. The adsorption capacity and adsorption affinity of NCF are founded greater than other adsorbent that have been mentioned in Table 1. The NCF is an efficient natural adsorbent for removing ferric ions from aquatic systems.

The effect of isotherm shape is discussed from the direction of predicting the weather and adsorption system is "favorable or "unfavorable". It was previously reported [45] that the dimensional analysis, separation factor, or equilibrium parameters "R_L" was as an essential feature of the Langmuir isotherm to predict adsorption system to be "favorable or "unfavorable" by Eq. (8):

$$R_L = 1/(1 + bC_i) \quad (8)$$

where C_i is the initial ferric ion concentration mg L^{-1}. The calculated R_L was 0.341, indicating for the favorable adsorption.

Furthermore, the apparent Gibbs free energy of sorption (ΔG°) is the fundamental criterion of spontaneity. Reaction occurs spontaneously at a given temperature if (ΔG°) is negative in value. The standard Gibbs free energy change (ΔG°) for the adsorption of ferric ion on the NCF surface can be calculated using the thermodynamic Eq. (9):

$$\Delta G^0 = -RT \ln k_L \quad (9)$$

where R is the universal gas constant (8.314 J/mol K), T is the absolute temperature in Kelvin, and b is the equilibrium constant, related to the Langmuir constant, b (= 0.0193).

Table 1
Adsorption isotherm of ferric ion onto NCF compared with similar reported studies

	Langmuir				Freundlich			Refs.
	q_{max} (mg g^{-1})	b (L mg^{-1})	ΔG	R^2	K_f	$1/n$	R^2	
Jordanian adsorbents								
Natural bentonite (NB)	20.96	0.005	−13.90	0.938	0.202	0.775	0.992	[12]
Natural quartz (NQ)	14.49	0.004	−13.40	0.961	0.115	0.780	0.996	[12]
Olive cake (OC)	58.48	0.015	−16.87	0.96	2.164	0.628	0.992	[10]
Natural zeolite (NZ)	7.35	0.014	−16.98	0.998	3.353	0.106	0.954	[8]
NCF	49.75	0.019	−17.59	0.993	1.114	0.840	0.997	This study
Others								
Carbon	6.14	0.274		1.00				[9,43]
Eggshells	5.991	1.285		0.983	3.0	0.608	0.959	[44]
Chitosan	90.09	2.413		0.999	55.3	0.301	0.982	[17]
Chitin	1.3982	0.259	−4.52	0.975	2.45	0.672	0.995	[15]

$$k_L = b \times M_A \quad (10)$$

where M_A is the molar weight of ferric ion, the calculated of equilibrium constant (k_L) equal 1077.809 L moL^{-1}.

The calculated of ΔG° is found to be −17.590 kJ moL^{-1} at 30 °C. This negative sign value shows the spontaneous nature for adsorbing ferric ion by the NCF adsorbent under this experiment conditions.

Freundlich model is commonly used to describe: (i) non ideal and reversible adsorption; and (ii) the adsorption characteristics of the heterogeneous surface [46]. The Freundlich equation does not consider all the sites on the adsorbent surface to be equal. Furthermore, it is assumed that, once the surface is covered, additional adsorbed species can still be accommodated (adsorbate–adsorbate interaction). In other words, the linearized Freundlich isotherm model is expressed as in Eq. (11), [47–48]:

$$\ln q_e = \ln K_f + \frac{1}{n} \ln C_e \quad (11)$$

The Freundlich constants K_f and n indicate the adsorption capacity and the adsorption intensity, respectively. They are calculated from the intercept and slope of the $\ln q_e$ versus $\ln C_e$ plot (see Fig. 9). It can be seen that the Freundlich model fitted the experimental data well, rather than a Langmuir isotherm model-based on its correlation coefficient value ($R^2 = 0.997$). This indicates for the heterogeneous assembly of ferric ions on the NCF surface. This is mainly due to the heterogeneity surface of NCF, which shown clearly in the K_d results as shown in Fig. 4. In this case, the Freundlich constants K_f and n were found to be 1.19 and 1.11, respectively. The magnitudes of K_f and n show easy separation of the aqueous ferric ion and they indicate favorable adsorption. The intercept K_f value is an indication of the adsorption capacity of the adsorbent; the slope $1/n$ indicates the effect of concentration on the adsorption capacity and represents adsorption intensity or surface heterogeneity [49–50]. It becomes more heterogeneous as its value gets closer to zero. A value below unity implies chemisorptions process [51]. As seen, the value of "n" was found high enough for separation. This model has been widely applied to describe the adsorption of ferric ions onto several adsorbents such as natural bentonite (NB) [12], natural quartz (NQ) [12], olive cake (OC) [10], and chitin [15] (see Table 1).

3.7. Kinetic modeling

In general, we have been talking about the effect of contact time on the adsorption process, which already have been described in Fig. 5. However, the importance of kinetic studies lies in the fact of controlling of adsorption mechanism in terms of sorption reaction and mass transfer steps. These two steps govern the transfer of ferric ions from the bulk of a solution to the binding active sites of the NCF adsorbent. The pseudo-first-order [52] and pseudo-second-order [53] models are applied to describe the kinetic behavior of ferric ion sorption. They are used to test the experimental batch data and identify the rate-controlling mechanism for the adsorption process.

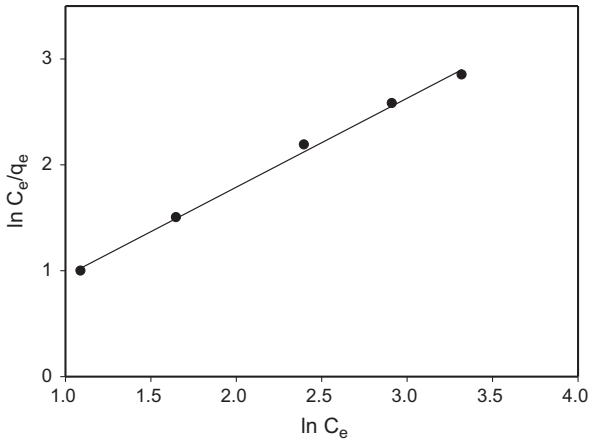

Fig. 9. The linearized Freundlich adsorption isotherms for adsorbing Fe^{3+} ion on NCF ($T = 30°C$; doses = 10 g L^{-1}; $C_i = 100$ mg L^{-1}; $t = 3$ h; and rpm = 300).

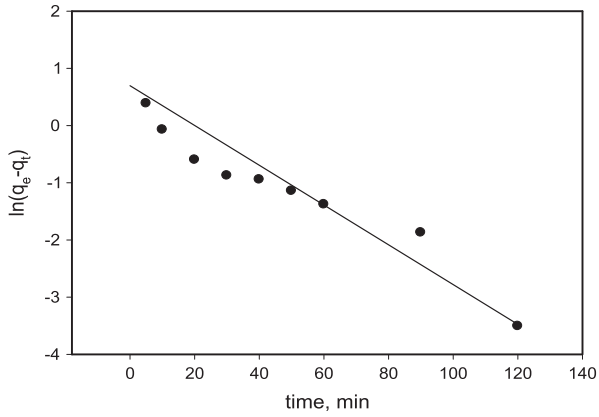

Fig. 10. Pseudo-first-order reaction for adsorbing Fe^{3+} ion on NCF ($T = 30°C$; doses = 10 g L^{-1}; $C_i = 100$ mg L^{-1}; $t = 3$ h; and rpm = 300).

The kinetics of the adsorption process can be studied by carrying out a separate set of adsorption time experiments at constant temperature (30°C), initial ferric ion concentration (100 mg L^{-1}), doses of the NCF ($S = 10$ g L^{-1}), and agitation speed (300 rpm).

The pseudo-first-order kinetic model and its integral can be expressed by Eq. (12) [52]:

$$\ln(q_e - q_t) = \ln q_e - k_1 t \quad (12)$$

where q_e and q_t (mg g^{-1}) are the amounts of adsorbed ferric ion at equilibrium and at times (t), respectively, k_1 (min^{-1}) is pseudo-first-order rate constant, and t (min) is the contact time of adsorption. The parameters k_1 and q_e can be determined by plotting $\ln(q_e - q_t)$ vs. t (see Fig. 10) to produce a straight line of slope (= k_1) and intercept (= $\ln q_e$), The values of k_1 and q_e are found at 0.0348 min^{-1} and 2.007 mg g^{-1}, respectively. The correlation coefficient ($R^2 = 0.826$) of the plot is found not good enough for the approval of the results. On comparing the calculated "q_e" value with that of experimental one (8.898 mg g^{-1}), we found that they are not compatible.

The pseudo-second-order equation is expressed by Eq. (13) [53]:

$$\frac{t}{q_t} = \frac{1}{k_2 q_e^2} + \frac{t}{q_e} \quad (13)$$

where k_2 is the rate constant of the pseudo-second order kinetic model(g mg^{-1} min^{-1}). The value of k_2 can be determined by plotting t/q_t vs. t (see Fig. 11) to obtain a straight line of slope $1/q_e$ and intercept of $1/(k_2 q_e^2)$. As shown, the values of k_2 and q_e are found 0.657 g/mg min and 8.93 mg g^{-1}, respectively. The correlation coefficient ($R^2 = 1.0$ (approx.)) of the plot is found good for approval the results. It can be seen that the calculated q_e is consistent with the experimental value ($q_e = 8.898$ mg g^{-1}).

The degree of goodness of a linear plot can be judged from the value of R^2 of the plot, which can also be regarded as a criterion in the determination of the adequacy of kinetic model. From the determination coefficient values above, the adsorption of ferric ion on NCF is regarded as pseudo-second-order rather than pseudo-first-order. This means that the ferric ion can be chemi-adsorbed by two sorption sites onto the NCF surface.

The kinetics results of this study are compared with other values as listed in Table 2. Apparently, the pseudo-second-order model is considered to be a rate

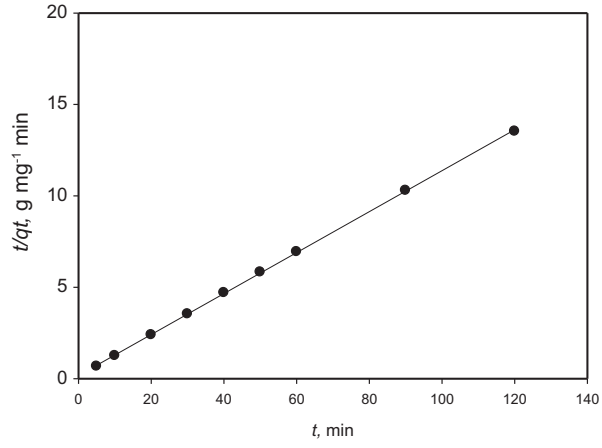

Fig. 11. Pseudo-second-order reaction for adsorbing Fe^{3+} ion on NCF ($T = 30°C$; doses = 10 g L^{-1}; $C_i = 100$ mg L^{-1}; $t = 3$ h; and rpm = 300).

Table 2
Adsorption kinetic of ferric ion onto NCF compared with similar reported studies

	Pseudo-first order		Pseudo-second order			Refs.
	k_1 (min^{-1})	R^2	k_2 ($g\,mg^{-1}\,min^{-1}$)	q_e	R^2	
Jordanian adsorbents						
Natural bentonite (NB)	0.066	0.89	0.337	0.649	0.99	[12]
Natural quartz (NQ)	0.057	0.76	0.552	0.746	0.99	[12]
Olive cake (OC)	0.061	0.89	0.018	15.97	0.99	[10]
Natural zeolite (NZ)	0.045	0.88	0.040	20.00	1.0	[8]
NCF	0.035	0.826	0.657	8.93	1.0	This study
Others						
Carbon			0.048	13.04	1.0	[9,43]
Eggshells			0.403	1.92	1.0	[44]
Chitosan	0.0306	0.96	0.032		1.0	[17]

limiting and controlling step. Where, similar results are observed using OC [10], NZ [8], NB [12], NQ [12], carbon [9,43], eggshells [44], and chitosan [17]. In general, we have found that the rate constant (k_2) is higher than what have been found in the recent studies (see Table 2).

The pseudo-first-order and pseudo-second-order kinetic models could not identify the diffusion mechanism. Thus, the diffusion of the ferric ion into the adsorbent pores can be determined by Weber–Moris intraparticle diffusion model [54]. This model was used in the form of Eq. (14):

$$q_t = k_{\text{int}}\, t^{0.5} + \text{C} \tag{14}$$

where C is constant, q_t is the amount of ferric ions adsorbed at a time ($mg\,g^{-1}$) and k_{int} is the intra-particle diffusion rate constant ($mg\,g^{-1}\,min^{-0.5}$). A plot of q_t versus $t^{0.5}$ giving straight line confirms an intra-particle diffusion of the sorption as shown in Fig. 12. The plot is not totally linear. This is indicative of some degree of boundary layer control and this further show that the intra-particle diffusion could not be the only mechanism involved. This plot presents multi-linearity which indicates that two or more steps to occur. The first, sharper portion (ca. $t^{0.5}$ range from 0 to 1.2375 $min^{0.5}$; i.e. from 0 to 5 min of adsorption period) is the external surface adsorption or instantaneous adsorption stage. The second portion is the gradual adsorption stage (ca. $t^{0.5}$ range from 2.236 to 4.4721 $min^{0.5}$; i.e. from 5 to 20 min of adsorption period), where the intraparticle

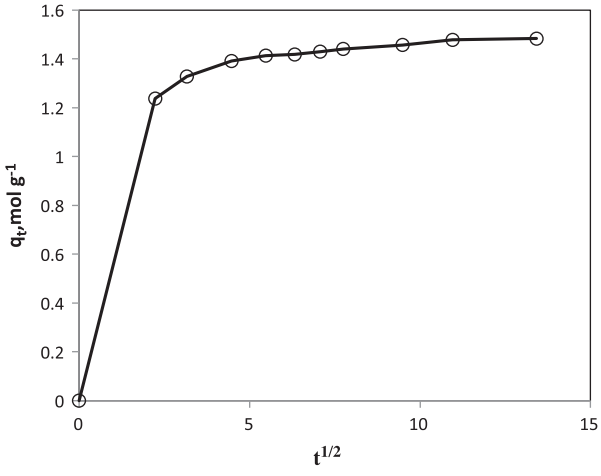

Fig. 12. Weber–Moris intra-particule diffusion kinetic model for adsorption of ferric ion on NCF starting from 0 to 180 min equilibrium contact time.

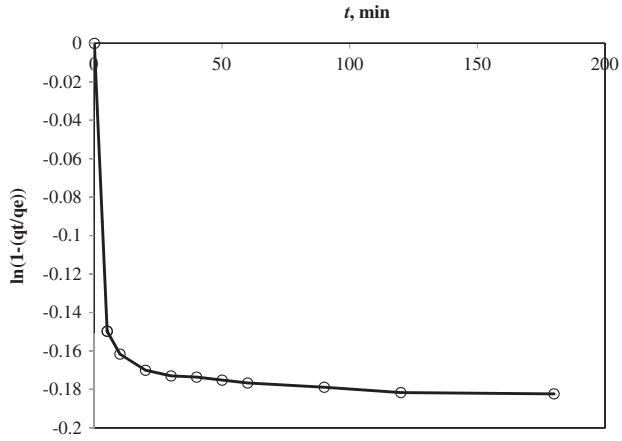

Fig. 13. Film diffusion mass transfer rate model of ferric ion on NCF that presented by Boyd et al.

diffusion is rate-controlled. The third portion is the final equilibrium stage where the intraparticle diffusion starts to slow down due to extremely low ferric ion concentrations in the solution and chemisorption stage is taken part on the NCF surface (which already has been successfully explained by pseudo-second-order kinetic model from 30 to 120 min of adsorption period).

Film diffusion mass transfer rate equation presented in Eq. (15) by Boyd et al. [55] is

$$\ln\left\{1-\frac{q_t}{q_e}\right\} = -k\,t \tag{15}$$

where k (min^{-1}) is the liquid film diffusion constant. A plot of $\ln\{1-\frac{q_t}{q_e}\}$ versus t should be a straight line with a slope $-k$ if the film diffusion is the rate limiting step. Fig. 13 shows the film diffusion mass transfer stage. Therefore, this stage cannot be considered as the rate controlling and limiting step.

4. Conclusion

NCF are found to be a very effective and low-cost adsorbent for adsorbing of aqueous ferric ions. The maximum removal has been found by applying several experimental parameters such as low concentration of ferric ion solution, high dosage of NCF, at 30°C. The final equilibrium of sorption starts after 120 min yielded a maximum removal of 90% (approx.). The equilibrium data have been yielded excellent fits within Langmuir and Freundlich isotherm models. The capacity (q_{max}) and intensity (b) of Langmuir adsorption are found 49.75 mg g^{-1} and 0.0193 L mol^{-1}, respectively. The capacity (K_f) and intensity ($1/n$) of Freundlich adsorption are 1.114 and 0.840, respectively. The results reveal that the adsorption of ferric ion on NCF is chemisorption, spontaneous and favorable in nature. The kinetic studies show that the adsorption rate is high, and is associated with uncontrolled rate during the first 5 min of adsorption. A kinetic model of the pseudo-second-order is good modeled to describe the adsorption rate of ferric ion onto the NCF surfaces. The adsorbing mechanism of the ferric ion can be spontaneously, favorably, and heterogeneously chemisorbed onto NCF adsorbent. Based on these thermodynamic and kinetic studies, we suggest applying this study to manage and prevent pollution of the aquatic system or to reclaim the water for reuse especially in the poor countries.

References

[1] P. Sarin, V.L. Snoeyink, J. Bebee, K.K. Jim, M.A. Beckett, W.M. Kriven, J.A. Clement, Iron release from corroded iron pipes in drinking water distribution systems: Effect of dissolved oxygen, Water Res. 38 (2004) 1259–1269.

[2] B. Das, P. Hazarika, G. Saikia, H. Kalita, D.C. Goswami, H.B. Das, S.N. Dube, R.K. Dutta, Removal of iron from groundwater by ash: A systematic study of a traditional method, J. Hazard. Mater. 141 (2007) 834–841.

[3] Warren Viessman Jr., M.J. Hammer, E.M. Perez, P.A. Chadik, Water Supply and Pollution Control, eight ed., Pearson Education International; Pearson Prentice Hall, Upper Saddle River, NJ, 2009.

[4] G.J. Kontoghiorghes, E.D. Weinberg, Iron: Mammalian defense systems, mechanisms of disease, and chelation therapy approaches, Blood Rev. 9 (1995) 33–45.

[5] W.C. Andersen, T.J. Bruno, Application of gas–liquid entraining rotor to supercritical fluid extraction: Removal of iron (III) from water, Anal. Chim. Acta 485 (2003) 1–8.

[6] D. Ellis, C. Bouchard, G. Lantagne, Removal of iron and manganese from groundwater by oxidation and microfiltration, Desalination 130 (2000) 255–264.

[7] H. Katırcıoglu, B. Aslım, A. Rehber Turker, T. Atıc, Y. Beyatl, Removal of cadmium(II) ion from aqueous system by dry biomass, immobilized live and heat-inactivated *Oscillatoria* sp. H1 isolated from freshwater (Mogan Lake), Bioresour. Technol. 99 (2008) 4185–4191.

[8] M. Al-Anber, Z. Al-Anber, Utilization of natural zeolite as ion-exchange and sorbent material in the removal of iron, Desalination 225 (2008) 70–81.

[9] A. Edwin Vasu, Adsorption of Ni(II), Cu(II) and Fe(III) from aqueous solution using activated carbon, E-J. Chem. 5 (2008) 1–9.

[10] Z. Al-Anber, M. Al-Anber, Adsorption of ferric ions from aqueous solution by olive cake: Thermodynamic and kinetic studies, J. Mex. Chem. Soc. 52 (2008) 108–115.

[11] P.S. Kumar, R. Gayathri, R.P. Arunkumar, Adsorption of Fe (III) ions from aqueous by Bengal gram husk powder: Equilibrium isotherms and kinetic approach, Electron. J. Environ., Agric. Food Chem. 9 (2010) 1047–1058.

[12] M. Al-Anber, Removal of high-level Fe^{3+} from aqueous solution using Jordanian inorganic materials: Bentonite and quartz, Desalination 250 (2010) 885–891.

[13] S. Bordoloi, S.K. Nath, R.K. Dutta, Iron ion removal from groundwater using banana ash, carbonates and bicarbonates of Na and K, and their mixtures, Desalination 281 (2011) 190–198.

[14] J.P. Vistuba, M.E. Nagel-Hassemer, F.R. Lapolli, M.Á. Lobo Recio, Simultaneous adsorption of iron and manganese from aqueous solutions employing an adsorbent coal, Environ. Technol. 34(2) (2013) 275–282.

[15] G. Karthikeyan, M.N. Andal, K. Anbalagan, Adsorption studies of Fe^{3+} on chitin, J. Chem. Sci. 117 (2005) 663–672.

[16] A. Burke, E. Yilmaz, N. Hasirci, O. Yilmaz, Iron(III) ion removal from solution through adsorption on chitosan, J. Appl. Polym. Sci. 84 (2002) 1185–1192.

[17] W.S. Wan, S. Ab. Ghani, A. Kamari, Adsorption behaviour of Fe(II) and Fe(III) ions in aqueous solution on chitosan and cross-linked chitosan beads, Bioresour. Technol. 96 (2005) 443–450.

[18] S.J. Kadolph, A.L. Langford, Textiles, eighth ed., Prentice-Hall, Upper Saddle River, NJ, 1998.

[19] B. F. Smith, I. Block. Textiles in Perspective, Prentice-Hall by Melissa Deffenbaugh, Englewood Cliffs, NJ, 1982.

[20] Y.-L. Lai, M. Thirumavalan, J.-F. Lee, Effective of heavy metal ions (Cu^{2+}, Pb^{2+}, Zn^{2+}) from aqueous solution by immobilization of adsorbents on Ca-alginate beads, Toxicol. Environ. Chem. 92 (2010) 697–705.

[21] A.A. Nada, N.A. El-Wakil, M.L. Hassan, A.M. Adel, Differential adsorption of heavy metal ions by cotton stalk cation-exchangers containing multiple functional groups, J. Appl. Polym. Sci. 101 (2006) 4124–4132.

[22] D. Zhoua, L. Zhang, J. Zhou, S. Guo, Cellulose/chitin beads for adsorption of heavy metals in aqueous solution, Water Res. 38 (2004) 2643–2650.

[23] H-T. Kim, K. Lee, Application of insoluble cellulose xanthate for the removal of heavy metals from aqueous solution, Korean Z Chem. Eng. 16 (3) (1999) 298–302.

[24] Sh. Liang, X.-Y. Guo, N.-Ch. Feng, Q.-H. Tian, Effective removal of heavy metals from aqueous solutions by orange peel xanthate, Trans. Nonferrous Met. Soc. China 20 (2010) s187–s191.
[25] N.A. Bagrovskay, O.V. Alekseev, O.V. Rozhkov, A.N. Rodionov, S.A. Lilin, Extracting heavy metals with cellulose-containing materials, Prot. Met. 44 (2008) 394–396.
[26] H. Vu-Manh, H.B. Öztürk, Th. Bechtold, Swelling and dissolution mechanism of regenerated cellulosic fibers in aqueous alkaline solution containing ferric–tartaric acid complex—Part II: Modal fibers, Carbohydr. Polym. 82 (2010) 1068–1073.
[27] H. Vu-Manh, H.B. Ozturk, T. Bechtold's, Swelling and dissolution mechanism of lyocell fiber in aqueous alkaline solution containing ferric tartaric acid complex, Cellulose 17(3) (2010) 521–532.
[28] E.E. Ergozhin, N.A. Bektenov, A.K. Mekebaeva, N.N. Chopabaeva, Preparation of phosphoric-carboxylic cation exchangers from wood cellulose, Chem. Nat. Compd. 39 (2003) 299–302.
[29] M. Hartzell-Lawson, Y.-L Hsieh, Characterizing the noncellulosics in developing cotton fibers, Text. Res. J. 70 (2000) 810–819.
[30] N. Kannan, T. Veemaraj, Removal of lead(II) ions by adsorption onto bamboo dust and commercial activated carbons -a comparative study, E-J. Chem. 6(2) (2009) 247–256.
[31] S.A. Khan, R. Ur-Reman, M.A. Khan, Adsorption of Cs(I), Sr (II) and Co(II) on Al_2O_3, J. Radioanal. Nucl. Chem. 207 (1996) 19–37.
[32] M. Balintova, A. Petrilakova, E. Singovszka, Study of metals distribution between water and sediment in the Smolnik creek (Slovakia) contaminated by acid mine drainage, Chem. Eng. Trans. 28 (2012) 73–78.
[33] D.S. Kim, Adsorption characteristics of Fe(III) and Fe(III)–NTA complex on granular activated carbon, J. Hazard. Mater. 106B (2004) 67–84.
[34] R. Donat, A. Akdogan, E. Erdem, H. Cetisli, Thermodynamics of Pb^{2+} and Ni^{2+} adsorption onto natural bentonite from aqueous solutions, J. Colloid Interface Sci. 286 (2005) 43–52.
[35] D. Xu, X.L. Tan, C.L. Chen, X. Wang, Adsorption of Pb(II) from aqueous solution to MX-80 bentonite: Effect of pH, ionic strength, foreign ion and temperature, Appl. Clay Sci. 41 (2008) 37–46.
[36] M. Al-Anber, Removal a Model Solution of Trivalent Iron Using Jordanian Natural Zeolites, Asian J. Chem. 19 (2007) 3493–3501.
[37] S. Babel, T.A. Kurniawan, Low-cost adsorbents for heavy metals uptake from contaminated water: A review, J. Hazard. Mater. B97 (2003) 219–243.
[38] V.J. Inglezakis, M.D. Loizidou, H.P. Grigoropoulou, Ion exchange studies on natural and modified zeolites and the concept of exchange site accessibility, J. Colloid Interface Sci. 275 (2004) 570–576.
[39] B.B. Johnson, Effect of pH, temperature and concentration on the adsorption of cadmium on goethite, Environ. Sci. Technol. 24 (1990) 112–118.
[40] M. Allawzi, S. Al-Asheh, H. Allaboun, O. Borini, Assessment of the natural jojoba residues as adsorbent for removal of cadmium from aqueous solutions, Desalin. Water Treat. 2(1–3) (2010) 60–65.
[41] I. Langmuir, The constitution and fundamental properties of solids and liquids, J. Am. Chem. Soc. 38 (1916) 2221–2295.
[42] M.M. Nassar, K.T. Ewida, E.E. Ebrahiem, Y.H. Magdy, M.H. Mheaedi, Adsorption of iron and manganese ions using low-cost materials as adsorbents, Adsorpt. Sci. Technol. 22 (2004) 25–37.
[43] Z. Zawani, C.A. Luqman, Th.S.Y. Choong, Equilibrium, kinetic and thermodynamic studies: Adsorption of removal black 5 on the palm kernel shell activated carbon (PKS-AC), Eur. J. Sci. Res. 37 (2009) 63–71.
[44] N. Yeddou, A. Bensmaili, Equilibrium and kinetic of iron adsorption by eggshells in a batch system: Effect of temperature, Desalination 206 (2007) 127–134.
[45] M. Al-Anber, Thermodynamics Approach in the Adsorption of Heavy Metals. Juan Carlos Moreno-Pirajan, Thermodynamics-Interaction Studies-Solids, Liquids and Gases Book, first ed., In-Tech, Rijeka, 2011, pp. 737–764, (Chapter 27). ISBN: 978-953-307-318-7.
[46] H.J. Butt, K. Graf, M. Kappl, Physics and Chemistry of Interfaces, Wiley-VCH, Weinheim, 2003, pp. 185–193.
[47] H. Freundlich, Über die adsorption in losungen [Adsorption in solution], Z. Phys. Chem. 57 (1906) 384–470.
[48] G.W. Van Loon, S.J. Duffy, Environmental Chemistry, second ed., Oxford University Press, New York, NY, 2005, pp. 308–318.
[49] D.G. Kinniburgh, Isotherm: A computer program for analyzing adsorption data. Report WD/ST/85/02. Version 2.2. British Geological Survey, Wallingford, England, 1985.
[50] D.G. Kinniburgh, General purpose adsorption isotherms, Environ. Sci. Technol. 20 (1986) 895–904.
[51] K.Y. Foo, B.H. Hameed, Insight into the modeling of adsorption isotherm systems, Chem. Eng. J. 156 (2010) 2–10.
[52] S. Lagergren, K.S. Vetenskapsakad, Zur theorie der sogenannten adsorption geloester stoffe, Kungliga Svenska Vetenskapsakad. Handl. 24 (1898) 1–39.
[53] Y.S. Ho, G. McKay, Pseudo-second order model for sorption processes, Process Biochem. 34 (1999) 451–465.
[54] W.J. Weber Jr., F.O. Digiano, Process Dynamics in Environmental System; Environmental Science and Technology Series, John Wiley and Sons, New York, NY, 1996, pp 89–94.
[55] G.E. Boyd, A.W. Adamson, L.S. Myers, The exchange adsorption of ions from aqueous solutions by organic zeolites, II. Kinetics. J. Am. Chem. Soc. 69(11) (1947) 2836–2848.